Reversing buoyancy of particle-driven gravity currents

Andrew J. Hogg
Centre for Environmental and Geophysical Flows, School of Mathematics, University Walk, Bristol BS8 1TW, United Kingdom

Herbert E. Huppert and Mark A. Hallworth
Institute of Theoretical Geophysics, Department of Applied Mathematics and Theoretical Physics, Silver Street, Cambridge CB3 9EW, United Kingdom

(Received 18 June 1998; accepted 21 May 1999)

Particle-laden flows exhibit reversing buoyancy behavior if the density of the ambient through which they propagate is greater than that of the interstitial fluid, though less than the initial bulk density of the suspension. In this case a gravity current is initiated above the underlying boundary until sufficient particles have sedimented from the flow, at which time the particle-laden fluid becomes less dense than the surrounding ambient. The buoyancy of the residual suspension reverses and it lifts off the boundary to ascend through the ambient. Such phenomena are encountered in industrial and natural situations. This study presents a laboratory investigation of finite volume releases of particle-laden fluid which undergo reversing buoyancy. A simple box model theory is proposed to describe the flow and to predict the distance from the source at which lift-off occurs. The predictions of the model agree well with both our experiments and those of previous studies. Additionally, we investigate these flows using the shallow-water equations which are analyzed using asymptotic series. These reveal the structure of the internal dynamics within the currents and predict lift-off distances which verify the validity of those obtained from the less rigorous box model. [S1070-6631(99)02309-0]

I. INTRODUCTION

When a suspension of particles is introduced into an ambient fluid, a variety of fluid mechanical phenomena may be observed depending upon the concentration and density of the suspended particles and the densities of the ambient and interstitial fluids. (The latter is sometimes known as the suspending fluid.) If the densities of the ambient and interstitial are identical then the presence of the relatively heavy particles makes the suspension more dense than the surrounding fluid. Hence there is a buoyancy-derived force which drives a boundary-hugging flow and the suspension is transported away from its source. The particles, however, continually sediment out of the current to the underlying boundary, thus reducing the density difference and the flow decelerates. Such turbidity currents are common features in lakes, oceans, and the atmosphere[1] and are important mechanisms for the transport of sedimentary particles.[2] If the density of the interstitial fluid is greater than that of the ambient the presence of the suspended particles adds to the overall excess density and similar phenomena are observed to those described above, with the additional feature that even after all the particles have settled out there is still a buoyancy force driving the flow. If, however, the density of the interstitial fluid is less than that of the ambient then the motion of the particle-laden fluid is determined by its initial bulk density. It could be buoyant relative to the ambient, in which case it rises as a particle-laden plume.[3] Conversely, if it is initially heavier than the ambient it will flow as a boundary-hugging gravity current until sufficient particles have sedimented out to render its bulk density less than the density of the surrounding fluid. At this point the current lifts-off the boundary and ascends through the ambient. Such reversing-buoyancy currents are found when fresh-water, sediment-laden turbidity currents enter saline oceanic waters[1] or when hot ash-laden pyroclastic flows are emitted from volcanic sources into cooler surrounding air and loft to form coignimbrite clouds.[4] Also, many industrial effluents are discharged as hot particulate mixtures into a cooler environment.

There have been a number of recent studies of particle-driven gravity currents which analyze the flows from both an experimental and theoretical viewpoint. These include two-dimensional and axisymmetric gravity currents generated by the release of a fixed volume;[5–9] currents generated by a constant flux of fluid and their interaction with topography;[10] erosional currents;[11] and studies of the influence of rotation and a background mean flow.[12,13] Currents which exhibit reversing-buoyancy phenomena have received some attention. Sparks *et al.*[14] performed experiments on releases of a finite volume of suspension of relatively heavy particles with relatively light interstitial fluid, whilst Hurzeler *et al.*[15] performed experiments on currents generated by constant volume fluxes. In this paper we report some additional experiments in which finite volumes of suspensions are released into an a quiescent ambient (see Sec. II). Sparks *et al.*[14] developed a theoretical description of the flow which employed a ''shallow-water'' model (as described further in Sec. V). These data were reconsidered by Hurzeler *et al.*[15] who employed a time-dependent, two-dimensional, numerical model to explain the observations as well as to present an empirical relationship for the temporal evolution of the current. This

empirical model is based upon dimensionless variables appropriate to the spreading of a compositional gravity current with the influence of particle sedimentation appearing as an experimentally determined function. We demonstrate that by a different choice of dimensionless variables and some asymptotic analysis of the governing equations, a different relationship may be derived. This new expression is consistent with the dynamics of the motion.

The motion of gravity currents has been described using a variety of mathematical models with a range of complexity.[2] The simplest models, which still yield considerable insight, employ dimensional analysis to determine how the run-out lengths and velocities depend upon the initial volume and buoyancy of the fluid and the settling velocity of the suspended particles. Box models provide a systematic means to perform such analysis.[7–9,16] They also yield quantitative predictions for the temporal evolution of the characteristics of the flow, generally in closed analytic form.[13] However, they do not provide information on the variations of velocity and concentration within the current. Such information does emerge, though, from ''shallow-water'' models[17] in which the flow is assumed to be predominantly horizontal and hydrostatic in the vertical. This is a considerable simplification of the full equations of motion and such models may be integrated numerically to find the distribution of height, velocity and concentration within the current. At the front of the current, though, the flow is not predominantly horizontal. Instead there are unsteady, three-dimensional motions. Benjamin[18] demonstrated how the velocity of the front of the current may be related to the relative depth of the flow through a Froude number and derived an expression which was later experimentally tested by Huppert and Simpson.[16] A final category of model with an increased level of complexity is numerical simulation of the flow by the integration of the full equations of motion. This avoids the need for a frontal boundary condition but requires the adoption of a scheme to parameterize the turbulent motions. Such an approach, although numerically intensive, has been successfully employed by Klemp *et al.*,[19] Xu and Moncrieff,[20] de Rooij *et al.*[21] and Hurzeler *et al.*[15] The first two of these studies treat the fundamental situation of a compositional gravity current driven solely by differences in density. The third considers gravity currents intruding along the interface between two fluid layers. The last paper treats a particle-driven gravity current with reversing buoyancy, and incorporates a number of complexities due to the interactions of particle and fluid motions.

In this paper we adopt the ''box'' model approach and demonstrate how to derive simple, analytical predictions of the lift-off distances of reversing buoyancy, particle-driven currents. The theory indicates that these distances are a function of the ratio of the density difference between the interstitial and ambient to the excess bulk density of the suspension (Sec. III). This analysis yields explicit analytical results which may be simply applied to industrial and natural settings. We re-evaluate the data of Sparks *et al.*[14] and indicate how these results fit in with more complex models (Sec. IV). In Sec. V we indicate how these dimensional scalings of the box model emerge from a ''shallow-water'' model and how asymptotic analysis may be applied to elucidate the structure of the flow within the current. Finally, we discuss (Sec. VI) some applications of this work and indicate some areas of future research. We also include an appendix which examines the evolution of currents which gradually progress from a regime in which their thickness is comparable to the depth of the ambient to a regime in which the thickness is small compared to the depth of the ambient.

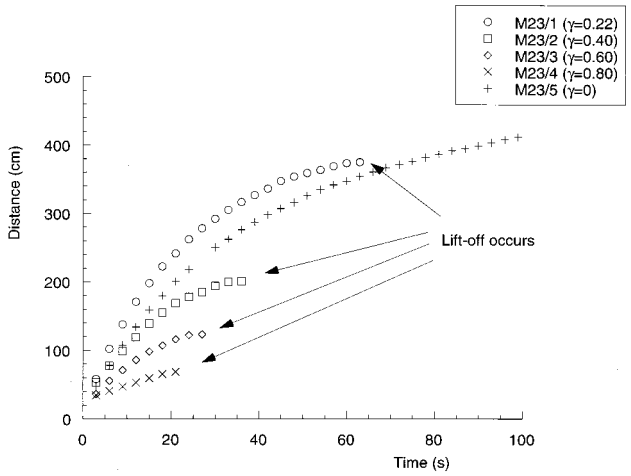

FIG. 1. The distance of the front of the gravity current from the source as a function of time. The five experimental runs correspond to different values of the parameter γ.

II. EXPERIMENTS

Sparks *et al.*[14] performed an experimental investigation of reversing-buoyancy currents in a 6 m long flume of width 20 cm with a depth of ambient fluid of 40 cm. Alumina particles of density 3.985 g cm^{-3} and mean diameter 67 μm were suspended in solutions of either aqueous methanol or fresh water, which were then released from a lock of length 20 cm into fresh or saline water, respectively. Both situations led to particle-driven gravity currents with reversing buoyancy. Sparks *et al.*[14] tracked the front of these currents and detected the distance at which they became buoyant and lifted off.

In our study experiments were performed in a 9.5 m long flume of width 25 cm with an ambient fluid depth of 20 cm. Suspensions of relatively monodisperse silicon carbide particles with mean diameter 23 μm and density 3.217 g cm^{-3} were employed. The interstitial fluid was aqueous methanol whilst the ambient was fresh water. The initial bulk density was adjusted by varying the initial mass loading of particles. The well-mixed suspension, to which a very small quantity of Calgon was added to remove coagulation effects, was released from a lock of length 10 cm. To initiate the current the lock-gate was removed rapidly and the frontal position was measured at intervals of 3 s until the current became buoyant and lifted off. The position of the front as a function of time is shown in Fig. 1 whilst the experimental parameters are given in Table I. In all of the experiments the lift-off occurred before viscous forces began to play a dominant role. Estimates of the Reynolds number of the currents suggest

TABLE I. Details of the experiments conducted in this study, giving the mass of methanol and 23 μm diameter particles added to 5180 g of water to make the initial suspension, and measurements of the postion and time of run-out. The ambient fluid in each case was fresh water. The settling velocity of an individual particle in the suspending fluid is 0.058 cm s^{-1} for fresh water and 0.048 cm s^{-1} for the water/methanol mixture.

Experiment	Mass of methanol (g)	Mass of particles (g)	Runout length (cm)	Runout time (s)
M23/1	575	659	375	63
M23/2	575	358	201	33
M23/3	575	237	123	27
M23/4	575	178	69	21
M23/5	0	237	496	210

that it is initially in excess of 1000 throughout the flow. The experiments supplement those of Sparks *et al.*[14] and our aim is to develop a theoretical description which encompasses all of them.

In these experiments, the lift-off distance is taken as the downstream distance at which the nose of the current first becomes buoyant, relative to the ambient fluid, and leaves the underlying boundary to ascend towards the free surface. No further propagation of the front of the current occurs along the bottom boundary. This distance may be clearly identified in each of the experiments. It is noteworthy, though, that in the rest of the current the reversal in buoyancy is not as clearly defined. The whole current thickens as its buoyancy is progressively reduced. This is in marked contrast to the behavior of particle-driven currents for which the interstitial fluid is identical to the ambient. These flows progressively thin as the particles sediment to the underlying boundary, whereas reversing-buoyancy currents ascend through the entire ambient after they have become buoyant at the nose.

III. BOX MODEL ANALYSIS

We develop a box model of the two-dimensional propagation of particle-driven gravity currents, following Dade and Huppert[7] and Hallworth *et al.*[13] Our analysis is based on the assumption that the dynamics are controlled by a balance of inertial and buoyancy forces. The densities of the interstitial and ambient fluids and the particles are denoted by ρ_i, ρ_a and ρ_p, respectively, and the volume fraction of particles by ϕ. The density of the current is hence given by

$$\rho_c=(\rho_p-\rho_i)\phi+\rho_i. \tag{1}$$

The initial volume fraction of particles is ϕ_0 and a dimensionless measure of the difference in densities between interstitial and ambient relative to the initial excess density of the current is given by

$$\gamma=\frac{\rho_a-\rho_i}{(\rho_p-\rho_i)\phi_0}. \tag{2}$$

For a particle-driven current to be of a reversing buoyancy nature, γ must be positive and less than unity. As shown below, its magnitude is crucial in determining the lift-off distance.

In accord with the usual box model approach, we treat the geometry of the current as an evolving rectangle of length L and height h. The validity of this major simplification (and the reasons for its success) have been discussed recently by Hogg *et al.*[22] The current is also assumed to be nonentraining. Hence conservation of mass yields

$$hL=A, \tag{3}$$

where A is the initial cross-sectional area or volume per unit width. At the front of the current we invoke the Froude number condition

$$\frac{dL}{dt}=\mathrm{Fr}[g(\rho_c-\rho_a)h/\rho_a]^{1/2}. \tag{4}$$

In this expression g is the gravitational acceleration and Fr is the frontal Froude number given by[16]

$$\mathrm{Fr}=\begin{cases}0.5(h/H)^{-1/3}, & h/H>0.075\\ 1.19, & h/H<0.075,\end{cases} \tag{5}$$

where H is the depth of the ambient fluid. The volume fraction of particles in suspension evolves as[23,24]

$$\frac{d\phi}{dt}=\frac{-v_s\phi}{h}, \tag{6}$$

where v_s is the settling velocity of an individual particle. This may be calculated using the Stokes formula if the particles are sufficiently small. Otherwise it may be experimentally determined or empirically calculated to take into account the (small) inertial drag (see, for example, Soulsby[25]). The sedimentation law (6) indicates that the volume fraction of particles within the current decreases as the current propagates. Lift-off occurs when the density of the current has become equal to the density of the ambient. At this point not only has the current become neutrally buoyant, but also its frontal speed has fallen to zero. Equivalently, this condition is given by $\phi=\gamma\phi_0$. We examine the theoretical predictions of lift-off in the two regimes of deep and shallow ambient fluid, corresponding to the two functional forms of the frontal Froude number.

A. Relatively deep ambient fluid

In this regime the Froude number is constant and equal to 1.19.[16] From (4) and (6) we find that

$$\frac{d\phi}{dL}=-\frac{v_s\phi}{\mathrm{Fr}\,h[(\phi-\gamma\phi_0)g_p'h]^{1/2}}, \tag{7}$$

where the reduced gravity is denoted by $g_p'=(\rho_p-\rho_i)g/\rho_a$. We introduce dimensionless variables $\psi=\phi/\phi_0$ and $\xi=L/L_\infty$, where

$$L_\infty=\left(\frac{5\,\mathrm{Fr}(g_p'\phi_0A)^{1/2}A}{v_s}\right)^{2/5}.$$

This lengthscale corresponds to the predicted runout length when there is no density difference between the ambient and interstitial fluids.[13] We find that (7) is transformed to

$$\frac{d\psi}{d\xi}=-\frac{5\psi\xi^{3/2}}{(\psi-\gamma)^{1/2}}. \tag{8}$$

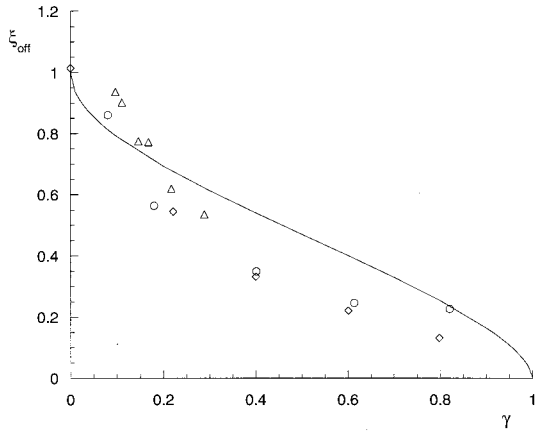

FIG. 2. The dimensionless lift-off distances (ξ_{off}) as a function of γ. The curve corresponds to the theoretical prediction of the box model while the symbols correspond to the experimental measurements (◇, M23/1-5; ○, K-O; △, C-I).

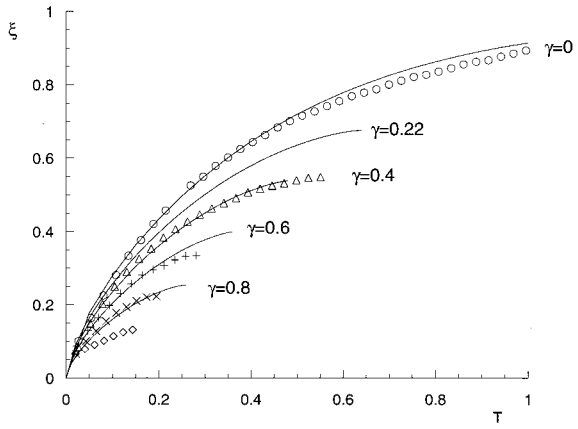

FIG. 3. The dimensionless distance from source as a function of dimensionless time. The symbols correspond to the experimental measurements, while the curves correspond to the box-model theory.

Lift-off occurs at $\psi=\gamma$ and so integrating this expression, we obtain the dimensionless lift-off distance, ξ_{off},

$$\xi_{\text{off}}^{5/2}=(1-\gamma)^{1/2}-\gamma^{1/2}\tan^{-1}[(1-\gamma)^{1/2}/\gamma^{1/2}]\equiv F(\gamma). \quad (9)$$

The lift-off distance, relative to the runout length when the densities of interstitial and ambient are equal, is purely a function of γ (Fig. 2). Note that $\xi_{\text{off}}=1$ at $\gamma=0$, which recovers the results of Hallworth *et al.*[13]

The rate at which the current approaches the lift-off length may be modeled continuing this simple approach. Adopting the dimensionless time scale $T=t/\tau$, where

$$\tau=\frac{5A}{v_s L_\infty}, \quad (10)$$

we find the following coupled, nonlinear differential equations model the temporal evolution of the length of the current and the concentration of particles within it,

$$\frac{d\psi}{dT}=-5\psi\xi, \quad (11)$$

$$\frac{d\xi}{dT}=\left(\frac{\psi-\gamma}{\xi}\right)^{1/2}. \quad (12)$$

These are integrated numerically subject to the boundary conditions $\psi=1$ and $\xi=0$ at $T=0$. Solutions of this system of equations are given in Fig. 3 for five different values of γ.

From these coupled differential equations, (11) and (12), we may construct approximate solutions for the temporal evolution of the dimensionless length and scaled volume fraction of particles. Such solutions may then be compared with the empirical spreading rules proposed by Hurzeler *et al.*[15] These solutions are essentially expansions in the regime $T\ll 1$. Nevertheless we find that they provide relatively good approximate solutions during a considerable portion of the evolution of the current. Carrying out considerable algebraic manipulations, we find that

$$\psi=1-3\left(\frac{3}{2}\right)^{2/3}(1-\gamma)^{1/3}T^{5/3}+O(T^{10/3}), \quad (13)$$

$$\xi=\left(\frac{3}{2}\right)^{2/3}(1-\gamma)^{1/3}T^{2/3}-\frac{1}{4}\left(\frac{3}{2}\right)^{7/3}(1-\gamma)^{-1/3}T^{7/3}+O(T^{12/3}). \quad (14)$$

In dimensional variables we find that

$$L(t)=c_1(1-\gamma)^{1/3}(g'A)^{1/3}t^{2/3}\times\left(1-c_2 t^{5/3}\frac{v_s(g'A)^{1/3}}{A(1-\gamma)^{2/3}}+O(t^{10/3})\right), \quad (15)$$

with $c_1=1.47$ and $c_2=0.11$ for Fr$=1.19$. Although the first term of this spreading law is similar (up to the numerical value of the constant c_1) to that proposed by Hurzeler *et al.*,[15] the second term is quite different. The constants c_1 and c_2 are purely functions of the Froude number at the front of the current. We demonstrate in See. V that this form of temporal evolution also emerges from the shallow-water model of the flow, and from that analysis the internal structure is explicitly calculated.

B. Relatively shallow ambient fluid

In this regime, the Froude number condition at the front of the current is given by Fr$=0.5(h/H)^{-1/3}$. Hence we find that

$$\frac{d\phi}{dL}=-\frac{2v_s\phi}{h((\phi-\gamma\phi_0)g_p'h)^{1/2}}\left(\frac{h}{H}\right)^{1/3}. \quad (16)$$

Once again this expression is rendered dimensionless by the introduction of the variables ψ and $\eta=L/L_*$, where

$$L_*=\left(\frac{13(g_p'\phi_0 A)^{1/2}A^{7/6}H^{1/3}}{v_s}\right)^{6/13}. \quad (17)$$

Similarly to above, this lengthscale corresponds to the predicted runout length when interstitial and ambient fluid are of identical density. Integrating this expression, we obtain the dimensionless lift-off distance

$$\eta_{\text{off}}^{13/6}=F(\gamma). \quad (18)$$

TABLE II. A summary of the experimental inputs and measurements of this study and of Sparks *et al.* (1993). The experimental, dimensionless lift-off, ξ_{off}, is calculated by dividing the measured lift-off length by L_∞ and by the empirical factor 1.6. The theoretical value of ξ_{off} is calculated from Eq. (9).

Experiment	d (μm)	ρ_p (g cm^{-3})	v_s (cm s^{-1})	ρ_a (g cm^{-3})	ϕ_0	$\rho_a-\rho_i$ (g cm^{-3})	H (cm)	Lift-off (cm)	γ	Expt. ξ_{off}	Theory ξ_{off}
C	67	3.985	0.65	1.01	0.020	0.010	40	377	0.17	0.77	0.72
D	67	3.985	0.67	1.0	0.015	0.005	40	390	0.08	0.86	0.81
E	67	3.985	0.62	1.0	0.015	0.010	40	263	0.18	0.56	0.71
G	67	3.985	0.47	1.0	0.023	0.028	40	197	0.40	0.35	0.54
H	67	3.985	0.40	1.0	0.030	0.054	40	157	0.61	0.25	0.39
I	67	3.985	0.44	1.0	0.038	0.094	40	145	0.82	0.23	0.24
K	67	3.985	0.65	1.01	0.012	0.010	40	234	0.29	0.53	0.62
L	67	3.985	0.65	1.01	0.015	0.010	40	287	0.22	0.61	0.68
M	67	3.985	0.65	1.01	0.023	0.010	40	390	0.15	0.77	0.74
N	67	3.985	0.65	1.01	0.030	0.010	40	482	0.11	0.90	0.78
O	67	3.985	0.65	1.01	0.035	0.010	40	516	0.10	0.94	0.79
M23/1	23	3.217	0.048	1.0	0.034	0.023	20	375	0.22	0.54	0.67
M23/2	23	3.217	0.048	1.0	0.019	0.023	20	201	0.40	0.33	0.54
M23/3	23	3.217	0.048	1.0	0.012	0.023	20	123	0.60	0.22	0.40
M23/4	23	3.217	0.048	1.0	0.009	0.023	20	69	0.80	0.13	0.26
M23/5	23	3.217	0.058	1.0	0.014	0.023	20	496	0	1.01	1.00

Once again the lift-off distance, relative to the runout when the densities of interstitial and ambient are identical, is purely a function of γ. It is also possible that during its evolution a current progresses from the regime of ''shallow'' to ''deep'' ambient fluid. This situation is modelled by matching together these two analyses, as presented in the Appendix.

IV. COMPARISON BETWEEN THEORY AND EXPERIMENTS

We now compare the box model theory for lift-off distance with the experimental results. The gravity currents studied in these experiments and in those of Sparks *et al.*[14] were generated by a lock-release. The relatively dense fluid therefore initially occupied the entire depth of the ambient. However, as the current propagated it became progressively thinner. The comparison between the predicted and the measured distances at which lift-off occurs should then be made using the combined theory of the Appendix. That analysis accounts for the transition between the different Froude number conditions. In this section, however, we assume that the ''deep'' ambient theory of Sec. III A may be employed. This considerably simplifies the presentation of the experimental results and has negligible effect upon their quantitative interpretation.

Comparison is made between the experimental results and the theoretical predictions of the lift-off distance given by (9) (see Fig. 2 and Table II). In the calculation of the runout length for particle-driven currents without reversing buoyancy, L_∞, we have had to include an empirical multiplicative constant of 1.6. This constant might be thought of in a number of ways. The rapid removal of the lock-gate leads to an initial slumping of dense, particle-laden fluid, during which some entrainmnet of ambient fluid occurs. This engulfment increases the bulk volume of the current, although the total buoyancy, $g_p\phi_0 A$ remains constant. Alternatively this constant might be thought of as a shape factor which accounts for the deviation of the profile of the current from the box-like shape which is assumed in the simple analysis. The inclusion of this factor of 1.6 has been shown to work well and to permit the experiments to be accurately predicted by a simple theory.[7] It has negligible effect upon the magnitude of γ, but must be included in the calculation of the time scale τ.

The settling velocity of both the silicon carbide and alumina particles of diameters 23 μm and 67 μm, respectively, are calculated using the Stokes' settling law with a kinematic viscosity appropriate to the interstitial fluid. Their Reynolds numbers, based on diameter and settling velocity, are less than unity and so inertial effects are negligible.

The comparison between the experimental results and the box model prediction is quite good (Fig. 2), given the assumptions underlying this model. There is, however, a systematic divergence between theory and experiments at low values of γ. These are currents which only become buoyant at distances close to the runout length of currents in the absence of reversing buoyancy. For such flows it is possible that entrainment of ambient fluid has begun to have an effect.[26,27] The mixing of ambient and interstitial fluid increases the density of the suspending fluid within the current. Thus for the current to become buoyant relative to the ambient, a greater proportion of the suspended particles must sediment out of the flow which postpones the point at which buoyancy reverses. The entrainment of ambient fluid is not included in this simple model, but nevertheless the box model has provided a simple conceptual tool for the analysis of reversing-buoyancy gravity currents. It has identified the two parameters γ and L_∞ (or L_*) as convenient means of classifying their evolution and making simple, analytical predictions of the lift-off distances.

We also compare the theory for the rate at which the current advances with the experimental measurements. In Fig. 3 the dimensionless position of the front, ξ, is plotted as a function of dimensionless time, T, for five different values

of γ. We note that the agreement between theory and experiment for currents in the absence of reversing buoyancy ($\gamma=0$) is very good. For nonzero values of γ the agreement is less good. This is primarily because the box model theory over-predicts the distance at which lift-off occurs. For example the measured dimensionless lift-off distance at $\gamma=0.22$ is 0.54 whereas theory predicts 0.67. Our calculations suggest that had this distance been accurately predicted then the temporal evolution towards lift-off would have been well modeled.

V. SHALLOW-WATER ANALYSIS

A. Nondimensionalization

The dynamics of gravity currents have often been mathematically modeled by the use of ''shallow-water'' theory.[5,17] These exploit the low aspect ratio of the flow and permit the hydrostatic approximation to be made in the vertical. Equations for the conservation of mass, momentum and volume fraction of particles are then given by

$$\frac{\partial h}{\partial t}+\frac{\partial}{\partial x}(uh)=0, \tag{19}$$

$$\frac{\partial}{\partial t}(uh)+\frac{\partial}{\partial x}\left(u^2h+\frac{1}{2}(\phi-\gamma\phi_0)g_p'h^2\right)=0, \tag{20}$$

$$\frac{\partial \phi}{\partial t}+u\frac{\partial \phi}{\partial x}=-\frac{v_s\phi}{h}, \tag{21}$$

where the height, velocity, and volume fraction of particles, denoted by h, u, and ϕ, are now functions of x and t. The boundary condition at the nose of the current is given by

$$\frac{du}{dt}=\mathrm{Fr}(g_p'(\phi-\gamma\phi_0)h)^{1/2} \quad \text{at } x=x_N(t), \tag{22}$$

where the nose is located at x_N. Finally, we assume that the total volume of fluid can be modeled as qt^α.[28] Thus, on the assumption that the flow is non-entraining, the volume is given by

$$\int_0^{x_N} h\,dx=qt^\alpha. \tag{23}$$

In this expression we have accounted for a temporally variable source of particle-laden fluid. (Note the important cases of $\alpha=0$ and $\alpha=1$, corresponding to constant volume and constant flux currents, respectively.) This system of equations may be rendered dimensionless by the introduction of the following dimensionless variables

$$X=x/l, \tag{24}$$

$$T=t/(v_s l/q)^{1/(\alpha-1)}, \tag{25}$$

$$H=h/(v_s^\alpha l/q)^{1/(\alpha-1)}, \tag{26}$$

$$U=u/(l^{\alpha-2}q/v_s)^{1/(\alpha-1)}, \tag{27}$$

where

$$l=(g_p'\phi_0)^{(\alpha-1)/(2\alpha-5)}q^{-3/(2\alpha-5)}v_s^{(\alpha+2)/(2\alpha-5)}. \tag{28}$$

The lengthscale, l, is the generalized runout length for the particle-driven gravity current. The adoption of this nondimensionalisation places all residual dimensionless ratios, other than γ, into the initial conditions. Numerical experimentation has found that the system of equations converges to a solution which is independent of the precise initial conditions, other than the volume of fluid released and its initial excess density, over a relatively short lengthscale.[22]

For the case of a constant volume release ($\alpha=0$), we find that

$$l=(g_p'\phi_0)^{1/5}q^{3/5}v_s^{-2/5}. \tag{29}$$

This is identical, up to a multiplicative constant, to the lengthscale L_∞ of Sec. III. For a constant flux current ($\alpha=1$), we find that

$$l=q/v_s. \tag{30}$$

Note that this lengthscale is independent of the initial reduced gravity of the particle-laden fluid.

As noted above, the adoption of this nondimensionalisation renders the governing equations free of any parameters other than γ. The distance at which lift-off occurs is then solely a function of γ, provided the current has evolved sufficiently so that the precise initial conditions do not influence the flow. This was confirmed by the numerical integration of the equations using a two-step Lax Wendroff scheme[5] until the volume fraction was reduced to $\phi_0\gamma$ at any point within the current. At this location, the flow has become buoyant relative to the ambient fluid. Numerical experimentation indicates that the location at which the buoyancy first reverses is within the tail of the current. Thereafter the shallow-water model of the flow is no longer valid, because the vertical fluid motions are no longer negligible. In Fig. 4(a), we plot the dimensionless position of the nose, $x_N(t)/l$, when lift-off occurs.

As reported by Sparks *et al.*[14] integration of the shallow-water equations up to this time leads to predictions of lift-off distance which are slightly too small for $\gamma\leqslant 0.1$ and slightly too large for $\gamma\geqslant 0.1$. We note that the box-model predictions of Secs. III and IV are prone to similar errors.

B. Asymptotic analysis

In the case of constant volume ($\alpha=0$), particle-driven gravity currents, Hogg *et al.*[22] have developed asymptotic series solutions to the shallow water Eqs. (19)–(21). These expansions exploit the small settling velocity of the particles relative to the initial velocity of the buoyancy-driven flow. They indicate how sedimentation of particles affects the flow and alters the dynamics from those of a compositional gravity current. Hurzeler *et al.*[15] have proposed empirical relationships for the spreading of reversing buoyancy currents based on dimensionless variables that are relevant to flows of compositional gravity currents. Their relationships include the effect of particle sedimentation via an empirical evaluation of the experimental data. In contrast, the asymptotic analysis presented below develops a theoretical model of this spreading and yields a different expansion. We show, how-

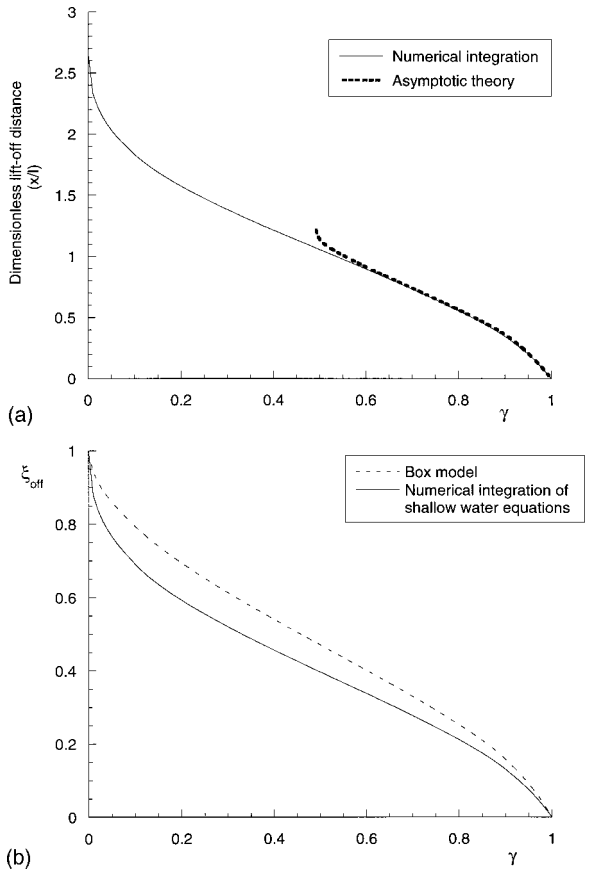

FIG. 4. (a) The dimensionless position of the nose of the current when the buoyancy first reverses. The solid line arises from numerical integration of the shallow-water equations (Sec. V A). The dotted line comes from the asymptotic theory of Sec. V B. (b) The lift-off distance, scaled by the maximum runout length of the particle-driven current when there is no buoyancy-reversal, as a function of γ. The solid curve comes from numerical integration of the shallow-water equations, while the dotted curve corresponds to the box model calculation.

ever, that this expansion, which emerges from the equations of motion, is also compatible with the experimental data.

In the absence of particle settling ($v_s=0$) for a current moving within a relatively deep ambient fluid so that the frontal Froude number is constant, the equations admit the following similarity solution[29]

$$x_{N0}=K[g_p'\phi_0 q(1-\gamma)]^{1/3}t^{2/3}, \tag{31}$$

$$u_0=\tfrac{2}{3}K[g_p'\phi_0 q(1-\gamma)]^{1/3}t^{-1/3}U_0(y), \tag{32}$$

$$h_0=\tfrac{4}{9}K^2 q[g_p'\phi_0 q(1-\gamma)]^{-1/3}t^{-2/3}H_0(y), \tag{33}$$

where the similarity variable is $y=x/x_{N0}$, the constant $K=[27\,\mathrm{Fr}^2/(12-2\,\mathrm{Fr}^2)]^{1/3}$ and the functions $H_0(y)$ and $U_0(y)$ are given by

$$H_0(y)=\frac{y^2-1}{4}+\frac{1}{\mathrm{Fr}^2} \quad \text{and} \quad U_0(y)=y. \tag{34}$$

The variables have the suffix 0 to indicate that they will form the first term of an asymptotic series. Following the concepts outlined in Hogg *et al.*,[22] we now consider a nonzero settling velocity and develop series expansions which show how the flow evolves from a homogeneous gravity current as a result of particle sedimentation. The dimensionless expansion parameter is given by[22]

$$\tau=\frac{v_s(g_p'\phi_0 q)^{1/3}t^{5/3}}{qK^2}. \tag{35}$$

Note that this is the dimensionless time proposed in (25) up to the constant factor of K^2. The leading-order expansion will be valid up to a critical value of τ. However, because the settling velocity is much less than the initial current velocity this corresponds to relatively long dimensional times. The study of Hogg *et al.*[22] was for the case of identical interstitial and ambient densities ($\gamma=0$). However their analysis may be extended by proposing the expansion series of the form

$$x_N=K[g_p'\phi_0 q(1-\gamma)]^{1/3}t^{2/3}[1+X_1\tau(1-\gamma)^{-2/3}+\cdots], \tag{36}$$

$$u=\tfrac{2}{3}K[g_p'\phi_0 q(1-\gamma)]^{1/3}t^{-1/3}[U_0(y)+\tau(1-\gamma)^{-2/3}U_1(y)+\cdots], \tag{37}$$

$$h=\tfrac{4}{9}K^2 q[g_p'\phi_0 q(1-\gamma)]^{-1/3}t^{-2/3}[H_0(y)+\tau(1-\gamma)^{-2/3}\times H_1(y)+\cdots], \tag{38}$$

$$\phi=1+\tau(1-\gamma)^{1/3}\phi_1(y)+\tau^2(1-\gamma)^{2/3}\phi_2(y)+\cdots. \tag{39}$$

Note that these expansions for $x_N(t)$ and $\phi(x,t)$ are qualitatively similar to the solutions of the box models (13) and (14). They entail identical groups of dimensional variables and proceed in identical powers of times. They differ, however, in the precise numerical value of the constants multiplying the dimensional groups. Such a difference, though, is not surprising given the assumptions underlying the ''box'' model.

By substituting these series into the governing equations and equating powers of τ, we can show that

$$\phi_1(y)=\frac{-27}{20H_0(y)} \tag{40}$$

and $X_1=-0.18$ for $\mathrm{Fr}=1.19$. The functions $H_1(y)$ and $U_1(y)$ satisfy a second-order, boundary-value differential equation and are given in Hogg *et al.*[22] This calculation reveals the structure of the internal dynamics of a particle-driven gravity current and provides an expression for the rate of propagation of the front of the current (36). It is found to be proportional to $t^{2/3}$ at very short times with a correction term proportional to $t^{7/3}$. In contrast, by the adoption of dimensionless variables which are appropriate to compositional gravity currents, Hurzeler *et al.*[15] propose an empirical expression for this rate of spreading. They suggest that

$$x_N=C_1[g_p'\phi_0 q(1-\gamma)]^{1/3}t^{2/3}\{1+C_2[tg_p'(1-\gamma)]^{1/2}\times q^{-1/4}+\cdots\}, \tag{41}$$

where C_1, C_2 are experimentally determined and C_2 is itself a function of settling velocity. While the first term of this expression is in agreement with (36), the second is different. We suggest that (36) is in fact the correct spreading rule.

At second-order the volume fraction is given by

$$\phi_2(y)=\left[\frac{729}{800H_0(y)^2}+\frac{27H_1(y)}{(1-\gamma)40H_0(y)^2}-\frac{27U_1(y)}{(1-\gamma)100H_0(y)^2}\frac{dH_0(y)}{dy}\right]. \quad (42)$$

Note that in this expression the factor of $(1-\gamma)$ does not appear uniformly in each of the terms. The distribution of particles arises from a combination of advection by the fluid and sedimentation through the current to the underlying boundary. These are related to the density difference between ambient and interstitial in different ways. At $O(1)$ the only effect of a density difference (i.e., nonzero γ) is to rescale the reduced gravity. However this is not so at $O(\tau)$ because the perturbation to the volume fraction involves a different power of $(1-\gamma)$ than the perturbations to the velocity and height. This arises because the first-order volume fraction is determined only by the leading-order height, while the first-order height and velocity fields are in balance with the pressure gradient associated with the density distribution within the flow. At $O(\tau^2)$ the lower order perturbation functions all contribute to the expansions and so expressions of the form (42) are found. We use these asymptotic series to calculate the position of the nose when the current first becomes buoyant. First, we establish the value of τ for which the volume fraction within the current first falls below γ. This value is then substituted into the spreading rule (36) to yield the lift-off distance. In Fig. 4(a), it may be noted that the asymptotic series gives excellent agreement with the numerical integration of the shallow-water equations up to $\gamma\approx 0.5$. For smaller values of γ, the asymptotic series diverges sharply from the numerics. It should be emphasized that these series are developed for the regime $\tau\ll 1$. Thus additional terms in the series may be required to model the evolution of the current at larger values of τ. These will be required for currents with $\gamma\ll 1$. Such currents run out over long distances and for long times before their buoyancy reverses. For such flows, we expect their rate of growth to be modeled by the inclusion of additional terms in the spreading law. Thus we expect $x_N=c_1t^{2/3}(1+c_2t^{5/3}+c_3t^{10/3}+\cdots)$, where c_1, c_2 and c_3 are appropriate constants. (See Hogg *et al.*[22] for a discussion of those values of τ for which the first-order terms in the series are sufficient to provide an accurate representation of the flow.)

To illustrate the use of this analysis we consider how the volume fraction evolves throughout the current for $\gamma=0.5$. Our analysis indicates that this is the smallest value of γ for which the leading-order solutions provide an adequate representation of the flow up to the point of buoyancy reversal. In Fig. 5 we plot the volume fraction, ϕ, as a function of the similarity variable, y, at times which correspond to $\tau=0$, 0.1, 0.2 and 0.37. At the final time plotted ($\tau=0.37$), the volume fraction has just fallen below γ. Hence the current has just become buoyant relative to the ambient at this time and so it lifts off. Note that the reversal in buoyancy first occurs in the tail of the current. Thereafter a shallow-water model of the flow is inappropriate because the horizontal lengthscales are no longer far in excess of the vertical lengthscales.

Finally we demonstrate that the spreading rule for the front of the current (36) is consistent with the experimental data. For example, we plot the length of the current as a function of time for experiment M23/1 in Fig. 6 and compare with it the asymptotic series of the form $c_1t^{2/3}(1-c_2t^{5/3})$. For this current, we find that $c_1=38\,\mathrm{cm\,s^{-2/3}}$ and $c_2=0.00044\,\mathrm{s^{-5/3}}$, while $\gamma=0.22$. We note that the comparison between the first-order series and the experimental data is fairly good, although is no better than the ''box'' model predictions. However, there is a clear indication that this series is being used beyond its domain of validity since there is a local maxima at $t\approx 50$. While additional terms in the series may be calculated, the domain of the first-order series may be simply extended by writing $x_N(t)=c_1t^{2/3}/(1+c_2t^{5/3})$. This truncated continued fraction provides an improved representation of the temporal dependence of the length of the current.

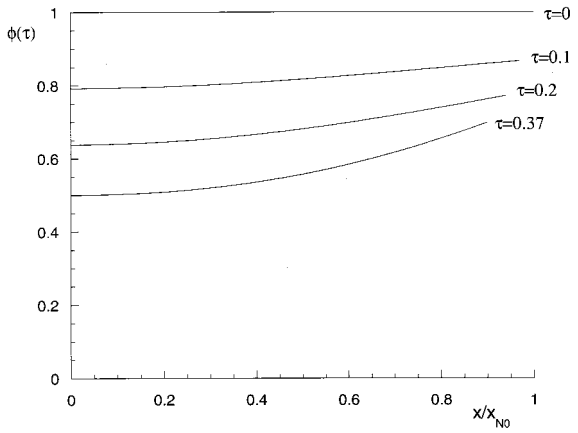

FIG. 5. The distribution of the volume fraction of particles within the current at various times for $\gamma=0.5$, calculated using asymptotic analysis. Note that the current has become buoyant relative to the ambient at $\tau=0.37$.

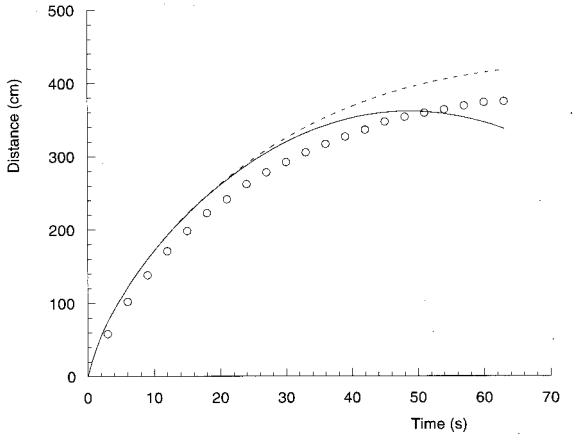

FIG. 6. The length of the current as a function of time ($\gamma=0.22$). The data points correspond to the experimentally measured positions; the solid curve to the spreading rule of the form $c_1t^{2/3}(1+c_2t^{5/3})$, where the constants c_1 and c_2 are theoretically determined; and the dotted curve to the spreading rule of the form $c_1t^{2/3}/(1-c_2t^{5/3})$.

VI. CONCLUSIONS AND APPLICATIONS

In this study we have performed laboratory experiments on particle-driven gravity currents which exhibit reversing buoyancy. We measured the rate of propagation of the current and the distance from the source at which the current becomes buoyant relative to the ambient fluid and ''lifts off.'' These experiments supplement those of Sparks *et al.*[14] We have developed a simple theory for the dependence of the lift-off distance upon the initial characteristics of the released fluid and suspended particles. It was shown to be convenient to calculate the lift-off distance, relative to the maximum run-out distance of a current for which the buoyancy did not reverse, as a function of γ. This parameter, γ, measures the density difference between the ambient and interstitial fluids relative to the initial excess density of the current due to the presence of the particles.

Gravity currents that exhibit reversing buoyancy occur as turbidity currents in which particles, suspended in relatively light coastal water, flow through deep oceanic waters. These currents are important mechanisms for the transport of sediment from the continental shelf into deep ocean basins. Reversing buoyancy currents also occur as pyroclastic flows from volcanic sources which loft to form coignimbrite clouds.[30] As a final example, they may also occur within an estuarine environment when sediment-laden, fresh water is discharged into saline water. Consider, for example, the discharge into an estuary of a relatively heavy, particulate pollutant which is suspended in fresh water. Typical values of the densities of the particulate and fluid phases are 3 $\mathrm{g\,cm^{-3}}$ and 1 $\mathrm{g\,cm^{-3}}$, while the saline estuary has a density of 1.02 $\mathrm{g\,cm^{-3}}$. We consider a volume of 1000 $\mathrm{m^3}$ which is discharged uniformly across a channel of width 10 m. The volumetric concentration of particulate is 0.05 and the particles have a settling speed of 0.1 $\mathrm{cm\,s^{-1}}$. If this current did not exhibit reversing buoyancy then the run-out distance of the current is 500 m. However, the interstitial fluid is less dense than the estuarine fluid and thus, as the particles sediment from the flow, the current eventually becomes buoyant relative to the ambient. For this scenario, γ is 0.2 and so the current is predicted to lift off after a distance of approximately 350 m. Predictions of the lift-off of flows of this nature may be simply determined from the ''box'' model analysis of this study. The method should provide a valuable tool for investigators studying environmental problems such as the dispersal of a pollutant or the transport of sediment.

Finally, we note that a future class of models for these flows of reversing buoyancy gravity currents could investigate the entrainment of ambient fluid;[27] a more complex description of the velocity field within the head of the flow; and a model of particle sedimentation which takes account of the relationship between the vertical distribution of particulate matter and the intensity of fluid turbulence.

ACKNOWLEDGMENTS

We thank with pleasure Steve Sparks and Jeremy Phillips for making their experimental data available. A.J.H. acknowledges financial support from the Nuffield Foundation.

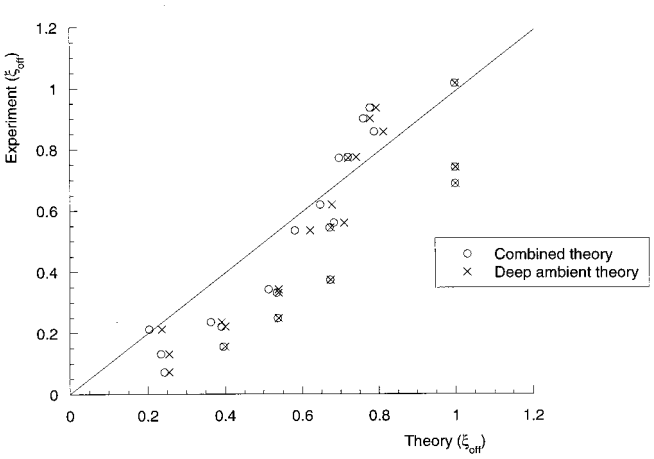

FIG. 7. Comparison between experimental measurements and theoretical predictions of the lift-off distance. Note that the theory using a Froude number condition at the front of the current which is a function of the depth of the current relative to the depth of the ambient fluid yields slightly improved agreement with the experimental data.

APPENDIX

The Froude number at the front of a current is a function of the depth of the current relative to that of the ambient flow [see Eq. (2)]. In laboratory studies of gravity currents generated by a lock-release of heavy fluid, it is possible for the current to propagate so that initially its depth relative to the ambient exceeds 0.075, but then in the latter stages its depth falls below this value. In this case the box model must account for both regimes. By adopting the dimensionless variables introduced in Sec. III A, we find that

$$\int_0^{\xi} \frac{5}{2} u^{3/2} f(u)\,du = F(\gamma), \tag{A1}$$

where

$$f(u) = \begin{cases} 1 & \text{for } u > x_* \\ 2\ \mathrm{Fr}(A/HL_\infty u)^{1/3}, & \text{for } u < x_*, \end{cases} \tag{A2}$$

$\mathrm{Fr}=1.19$ and $x_* = A/(0.075HL_\infty)$. Hence we find that

$$\xi_{\mathrm{off}} = \begin{cases} [13F(\gamma)x_*^{-1/3}/15]^{6/13}, & \text{for } \xi < x_* \\ [F(\gamma) - (2x_*^{5/2}/13)]^{2/5}, & \text{for } \xi > x_*. \end{cases} \tag{A3}$$

We compare the theoretically predicted and experimentally determined dimensionless lift-off distances in Fig. 7. We find that this ''combined'' theory has slightly improved the correspondence between theoretical and experimental results.

[1] J. E. Simpson, *Gravity Currents in the Environment and the Laboratory* (Cambridge University Press, Cambridge, 1997), p. 244.
[2] H. E. Huppert, ''Quantitative modeling of granular suspension flows,'' Philos. Trans. R. Soc. London, Ser. A **356**, 2471 (1998).
[3] S. N. Carey, H. Sigurdsson, and R. S. J. Sparks, ''Experimental studies of particle-laden plumes,'' J. Geophys. Res. **93**, 15314 (1988).
[4] R. S. J. Sparks, M. I. Bursik, S. N. Carey, J. S. Gilbert, L. S. Glaze, H. Sigurdson, and A. W. Woods, *Volcanic Plumes* (Wiley, New York, 1997).
[5] R. T. Bonnecaze, H. E. Huppert, and J. R. Lister, ''Particle-driven gravity currents,'' J. Fluid Mech. **250**, 339 (1993).
[6] R. T. Bonnecaze, M. A. Hallworth, H. E. Huppert, and J. R. Lister, ''Axisymmetric particle-driven gravity currents,'' J. Fluid Mech. **294**, 93 (1995).

[7]W. B. Dade and H. E. Huppert, ''Predicting the geometry of channelized deep-sea turbidites,'' Geology **22**, 645 (1994).
[8]W. B. Dade and H. E. Huppert, ''A box model for nonentraining suspension-driven gravity surges on horizontal surfaces,'' Sedimentology **42**, 453 (1995).
[9]W. B. Dade and H. E. Huppert, ''Runout and fine-sediment deposits of axisymmetric gravity currents,'' J. Geophys. Res. **100**, 18597 (1995).
[10]A. W. Woods, M. I. Bursik, and A. V. Kurbatov, ''The interaction of ash flows with ridges,'' Bull. Volcan. **60**, 38 (1998).
[11]G. Parker, Y. Fukushima, and H. M. Pantin, ''Self-accelerating turbidity currents,'' J. Fluid Mech. **171**, 145 (1986).
[12]M. Ungarish and H. E. Huppert, ''The effects of rotation on axisymmetric particle-driven gravity currents,'' J. Fluid Mech. **362**, 17 (1997).
[13]M. A. Hallworth, A. J. Hogg, and H. E. Huppert, ''Effects of external flow on compositional and particle gravity currents,'' J. Fluid Mech. **359**, 109 (1998).
[14]R. S. J. Sparks, R. T. Bonnecaze, H. E. Huppert, J. R. Lister, M. A. Hallworth, H. Mader, and J. C. Phillips;, ''Sediment-laden gravity currents with reversing buoyancy,'' Earth Planet. Sci. Lett. **114**, 243 (1993).
[15]B. E. Hurzeler, G. N. Ivey, and J. Imberger, ''Spreading model for a turbidity current with reversing buoyancy from a constant-volume release,'' Mar. Freshwater Res. **46**, 393 (1995).
[16]H. E. Huppert and J. E. Simpson, ''The slumping of gravity currents,'' J. Fluid Mech. **99**, 785 (1980).
[17]J. W. Rottman and J. E. Simpson, ''Gravity currents produced by instantaneous releases of heavy fluid in a rectangular channel,'' J. Fluid Mech. **135**, 95 (1983).
[18]T. B. Benjamin, ''Gravity currents and related phenomena,'' J. Fluid Mech. **88**, 223 (1968).
[19]J. B. Klemp, R. Rotunno, and W. C. Skamarock, ''On the dynamics of gravity currents in a channel,'' J. Fluid Mech. **269**, 169 (1994).
[20]Q. Xu and M. W. Moncrieff, ''Density current circulations in shear flows,'' J. Atmos. Sci. **51**, 434 (1994).
[21]F. de Rooij, P. F. Linden, and S. B. Dalziel, ''Saline and particle-driven interfacial intrusions,'' J. Fluid Mech. **389**, 303 (1999).
[22]A. J. Hogg, M. Ungarish, and H. E. Huppert, ''Particle gravity currents: Asymptotic solutions and box models,'' Euro. J. Mech. (to be published).
[23]H. M. Pantin, ''Interaction between velocity and effective density in turbidity flow: Phase-plane analysis, with criteria for autosuspension,'' Mar. Geol. **31**, 59 (1979).
[24]D. Martin and R. Nokes, ''Crystal settling in a vigorously convecting magma chamber,'' Nature (London) **332**, 534 (1988).
[25]R. L. Soulsby, *Dynamics of Marine Sands* (Thomas Telford, New York, 1998).
[26]M. A. Hallworth, ''Laboratory investigations of geological fluid flows,'' Ph.D. thesis, Anglia Polytechnic University, 1998.
[27]M. A. Hallworth, H. E. Huppert, J. C. Phillips, and R. S. J. Sparks, ''Entrainment into two-dimensional and axisymmetric turbulent gravity currents,'' J. Fluid Mech. **308**, 289 (1996).
[28]H. E. Huppert, ''The propagation of two-dimensional and axisymmetric viscous gravity currents over a rigid horizontal surface,'' J. Fluid Mech. **121**, 43 (1982).
[29]D. P. Hoult, ''Oil spreading on the sea,'' Annu. Rev. Fluid Mech. **2**, 341 (1972).
[30]R. S. J. Sparks, C. J. Rice, and J. G. Moore, ''The giant eruption cloud of May 18th, 1980, explosive eruption of Mount St. Helens, Washington,'' J. Volcanol. Geotherm. Res. **28**, 257 (1986).